Journal of Applied Polymer Science

Prediction of Long-Term Mechanical Properties of PVDF/$BaTiO_3$ Nanocomposite

Vahabodin Goodarzi, Mehrdad Kokabi, Mehdi Razzaghi Kashani, Ahmad Reza Bahramian
Polymer Engineering Department, Faculty of Chemical Engineering, Tarbiat Modares University, Tehran, Islamic Republic of Iran
Correspondence to: M. Kokabi (E-mail: mehrir@modares.ac.ir)

ABSTRACT: Low elastic modulus of polyvinylidene fluoride (PVDF) is a major drawback that can be compensated by adding nanoparticles. This work reports the long-term mechanical behavior of PVDF nanocomposite containing $BaTiO_3$ nanoparticle that is evaluated by creep test. The nanocomposite morphology was characterized by scanning and transmission electron microscopy techniques. The dynamic mechanical analysis (DMA) was employed to study the viscoelastic behavior of nanocomposite in a wide range of temperatures and frequencies. According to the creep tests, nanocomposite reduced the rate of the creep compliance at different temperatures. Moreover, the creep compliance for the nanocomposite sample decreased slightly in comparison with neat PVDF. Comparing the Burger's model and experimental results, the elastic and viscous parameters revealed the exactly opposite behavior with increasing temperature. The effect of frequencies on storage moduli of samples was investigated based on time–temperature superposition (TTS) method. © 2014 Wiley Periodicals, Inc. J. Appl. Polym. Sci. **2014**, *131*, 40596.

KEYWORDS: composites; conducting polymers; morphology; nanoparticles; nanowires and nanocrystals; viscosity and viscoelasticity

Received 25 September 2013; accepted 13 February 2014
DOI: 10.1002/app.40596

INTRODUCTION

Preparation of sensor and actuator elements is very important due to their wide applications in various aspects of human life. Many materials such as piezoelectric ceramics and polymers have been used as sensor and actuator elements. Piezoelectric ceramics have excellent electrical and mechanical properties, but poor processability characteristics. Polymers and ceramics are inherently viscoelastic and elastic, respectively. Therefore, the mechanical properties of polymer ceramic composites change by time and temperature.

In recent decades, much attention has been paid to the utilization of smart elements based on PVDF, due to its low cost and excellent formability.[1] In addition, much research has been done on how to determine the viscoelastic behavior of PVDF. Castagnet et al. studied the viscoelastic behavior of PVDF under different temperatures and stress conditions and showed that the material properties are functions of temperature and applied stress.[2] A similar result was obtained for polarized PVDF film as was reported by Mano et al.[3] They observed that polymer chains, connected by crystalline zones, have an important role in controlling the creep behavior at large deformation.[3]

Some researchers have recently tried to incorporate nanoparticles in PVDF to make nanocomposites. Achaby et al.[4] prepared PVDF nanocomposites with various types of nanoclay and they studied the formation of the crystalline structures of PVDF in the presence of nanoclay. Zak et al.[5] and Tang et al.[6] investigated the dielectric behavior of PVDF nanocomposites as a thin film prepared with nanoparticles of PZT and MWCNT. They reported that, introduction of nanoparticles to the polymer matrix plays a positive role in the enhancement of dielectric properties of nanocomposite systems. Rekik et al.[7] did similar studies on dielectric and crystallization behavior of PVDF/TiO_2 nanocomposites. They reported that the TiO_2 nanoparticle increases the dielectric constant while it decreases degree of crystallinity in PVDF.

Very few studies have been found on morphology of PVDF/$BaTiO_3$ nanocomposites. Dang et al.[8] showed $BaTiO_3$ nanoparticles are inclined to adsorb on the macromolecules of PVDF and create a suitable morphology. The nanostructures of $BaTiO_3$ in PVDF were examined by TEM. Mendes et al.[9] presented the thermal and electrical properties of PVDF/$BaTiO_3$ nanocomposites. They reported that the introduction of $BaTiO_3$ nanoparticles to PVDF enhances the dielectric and thermal degradation properties, which is a sign of probable appropriate compatibility between polymer and nanoparticles.

There are some limited studies on prediction of long-term mechanical properties of nanocomposites. Tang et al.[10] studied the effect of pristine and metal nanoparticles functionalized MWCNTs on the creep behavior of PVDF nanocomposites.

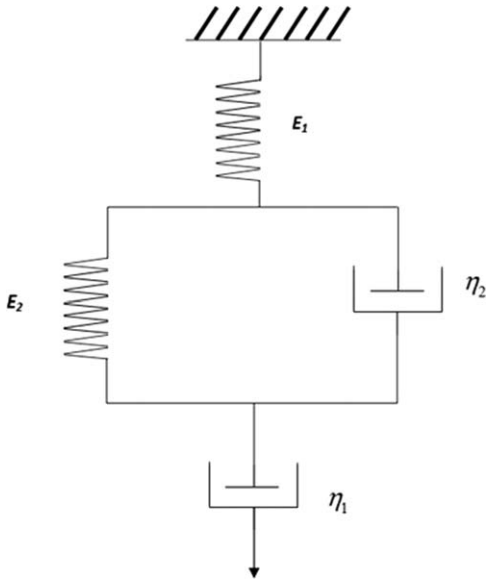

Figure 1. Burger model used to represent viscoelastic behavior.

They observed that functionalized MWCNTs reduced the creep compliance decay of PVDF nanocomposites versus time.

This study was aimed at predicting the long-term creep properties of solution casted PVDF/$BaTiO_3$ nanocomposite utilized in sensor element fabrication. Using time-temperature superposition (TTS) equation, a master curve was obtained to predict the creep compliance of samples. The viscoelastic parameters of the samples were determined comparing the experimental data with the Burger's model. On the other hand, by implementing frequency sweep at various temperatures, a master-curve was built for the storage modulus. The obtained results were used for predicting the long-term properties of the systems at various service conditions.

Theoretical Backgrounds

In the creep test, the applied stress (σ_c) is kept constant and the strain rate ($\varepsilon(t)$) is measured. Because of its viscoelastic nature, the polymeric material exhibits a combination of elastic and viscous characteristics when a force is applied. For the better presentation of creep behavior, the creep compliance $J(t)$ is used according to eq. (1).

$$J(t)=\frac{\varepsilon(t)}{\sigma_c} \tag{1}$$

A great number of models have been proposed to analyze the creep behavior of polymers, which can be used to achieve the viscoelastic parameters and predict polymers behavior. Maxwell and Voigt models are the simplest ones. The models consist of a spring with a modulus of E and a dashpot with a viscosity of η as elastic and viscous elements, respectively. In addition, parallel and series configurations of these two elements with respect to each other could generate Voigt and Maxwell models, respectively.[11] However, these models are weak to predict the viscoelastic properties via fitting the time dependent experimental data. It has been led to propose developed models by combining Maxwell and Voigt models in various configurations.[12] By combining Maxwell and Voigt models in a series form, a new four-element model namely the Burger's model is generated (Figure 1):

In the Burger's model, total strain can be determined from the following equations[12]:

$$\varepsilon=\varepsilon_1+\varepsilon_2+\varepsilon_3 \tag{2}$$

$$\varepsilon=\frac{\sigma_c}{E_1}+\frac{\sigma_c}{E_2}\left(1-\exp\left(-\frac{t}{\tau}\right)\right)+\frac{\sigma_c}{\eta_1}t \tag{3}$$

In eq. (2) ε, ε_1, ε_2 and ε_3 are the strains of the Burger, Maxwell spring, Maxwell dashpot and Kelvin unit. In eq. (3) E_1 and η_1 are the modulus and viscosity of the Maxwell spring and dashpot, respectively; E_2 and η_2 are the modulus and viscosity of the Kelvin spring and dashpot, respectively. Also in this equation σ_c and t are applied stress and creep test time, respectively. The eq. (3) is normalized with respect to the applied stress. According to the Burger's model, the viscoelastic parameters are determined by using eq. (3). The retardation time (τ) is very important parameter in determining viscoelastic behaviors and it is defined by the following equation:

$$\tau=\frac{\eta_2}{E_2} \tag{4}$$

If eq. (2) is divided by the applied stress, the creep compliance can be expressed as follows:

$$J=J_1+J_2\left(1-\exp\left(-\frac{t}{\tau}\right)\right)+\frac{t}{\eta_1} \tag{5}$$

In order to predict the creep behavior of polymers, a generalized Burger's model can be used.[13] This model can be extended to a more general case, consisting of n number of Maxwell and Voigt models as follows:

$$J(t)=J_0+\frac{t}{\eta_0}+\int_0^\infty J(\tau)\left(1-\exp\left(-\frac{t}{\tau}\right)\right)d\tau \tag{6}$$

where J_o and η_o are the initial creep compliance and viscosity, respectively.

Time-Temperature Superposition Equation

The prediction of long-term behavior of viscoelastic materials can be studied by time-temperature superposition (TTS) equation.[14] The creep test is one of the most effective way to determine the long-term mechanical properties of polymer materials. However, its high costs, as well as time concerns limit the use of this method. In TTS, the time shift factor is defined as a_T that can be determined from the following equation[14]:

$$\log a_T=\log\frac{t}{t_T} \tag{7}$$

where t and t_T are actual time and shifted time of creep test, respectively. By using this method, the transient long-term creep compliance master curve can be obtained from the short-term creep tests at a range of temperatures. Made by TTS at longer creep time than the individual short time creep curves, the master curve is accessible by practical experiments. The transfer parameter a_T is an important parameter in TTS that can be obtained through several methods. The WLF equation is the common tool as expressed by eq. (8)[11]:

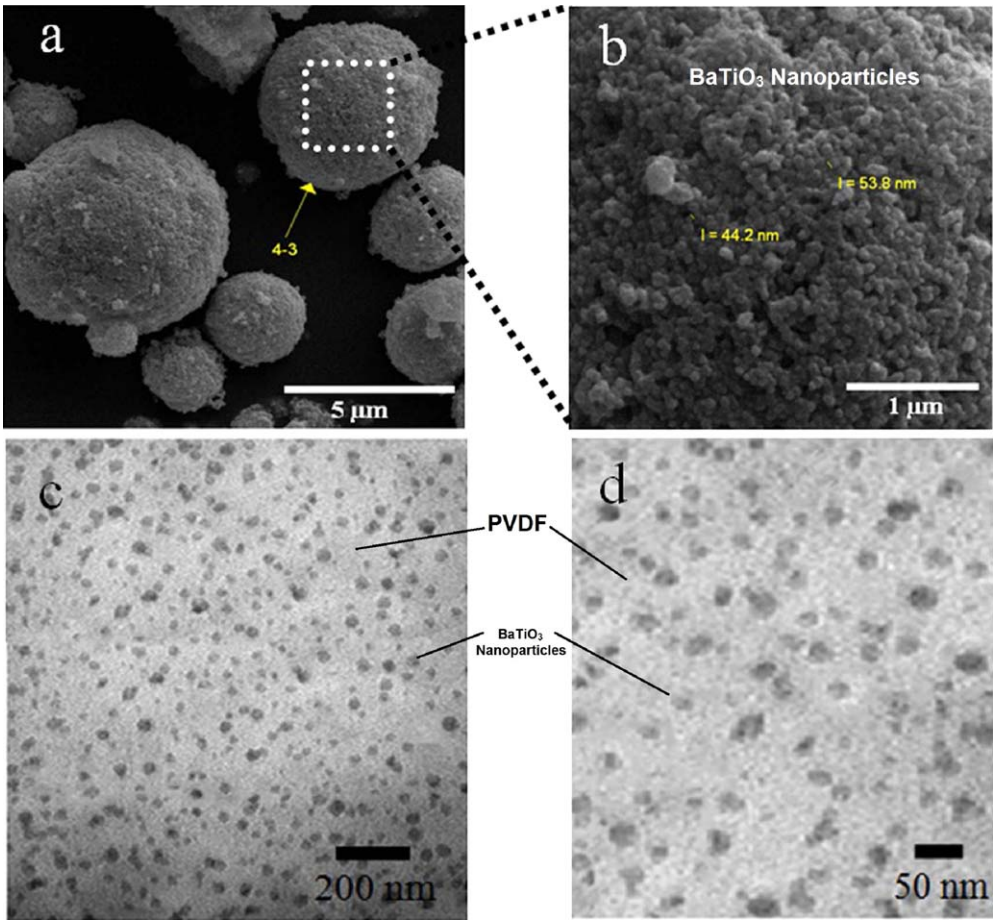

Figure 2. (a) and (b) SEM image of $BaTiO_3$ nanoparticles and (c) and (d) TEM image of PVDF/$BaTiO_3$ nanocomposite. [Color figure can be viewed in the online issue, which is available at wileyonlinelibrary.com.]

$$\log a_T = \frac{-C_1(T-T_0)}{C_2+(T-T_0)} \tag{8}$$

where $C_1 = -7.71$ and $C_2 = 116.6$ are constant parameters and T_o is the reference temperature and specific conditions for using these parameters are in the temperature range T_g to $T_g + 100^{\circ}C$.[11] This equation can be used for temperatures higher than T_g. For the higher temperatures than the reference temperature (T_o), the curve is shifted to the right with a negative shift factor ($\log a_T < 0$) and for lower temperatures the curve is shifted to the left with a positive shift factor ($\log a_T > 0$). Temperature $30^{\circ}C$ was considered as the reference temperature in this study.

To obtain a master curve, the time shift factor (a_T) for reference temperature of $30^{\circ}C$ can be determined from the eq. (8) and shifted time (t_T) coefficient can be estimated from eq. (7). Therefore, the master curve for reference temperature of 30°C in different temperature for each test can be achieved based on shifted time coefficient.

EXPERIMENTAL

Materials and Methods

The laboratory grade PVDF powder was supplied by Sigma-Aldrich (USA) with an average molecular weight of 534 kg/mol. $BaTiO_3$ nanoparticles (99.9% purity with an average diameter less than 100 nm) were purchased from Sigma-Aldrich (USA). Additionally, DMF solvent with a purity of 99.99% was obtained from Merck (Germany).

Sample Preparation

In this research, samples were prepared in the form of films. In order to have a homogeneous film, a 30 wt % solution of polymer was prepared. At first, the PVDF powder was dissolved in the DMF solvent using a magnetic stirrer at 300 rpm for 12 h in the ambient temperature ($25^{\circ}C$) to obtain a completely transparent and homogenous solution. These conditions ($25^{o}C$ and 12 h) are selected to prevent degradation of the PVDF macromolecules under heat and shear mixing. Using adhesive tapes, a mold was prepared on a glass plate with a width of 6 cm. Then, the polymer solution was cast in the prepared mold and then a film applicator was used to make a homogenous film. This technique prevents the creak formation in the polymer films. Next, the solvent was extracted from the casted films employing a vacuum oven at $40^{\circ}C$ for 12 h. The final film thickness was 40 μm. $BaTiO_3$ nanoparticles were added to the DMF and magnetically stirred at 1200 rpm for 12 h at room temperature, and then ultra-sonicated at 200 W for 1 h. This process was used for proper dispersion of $BaTiO_3$ nanoparticles in the DMF solvent to prevent formation of agglomerates and create desirable

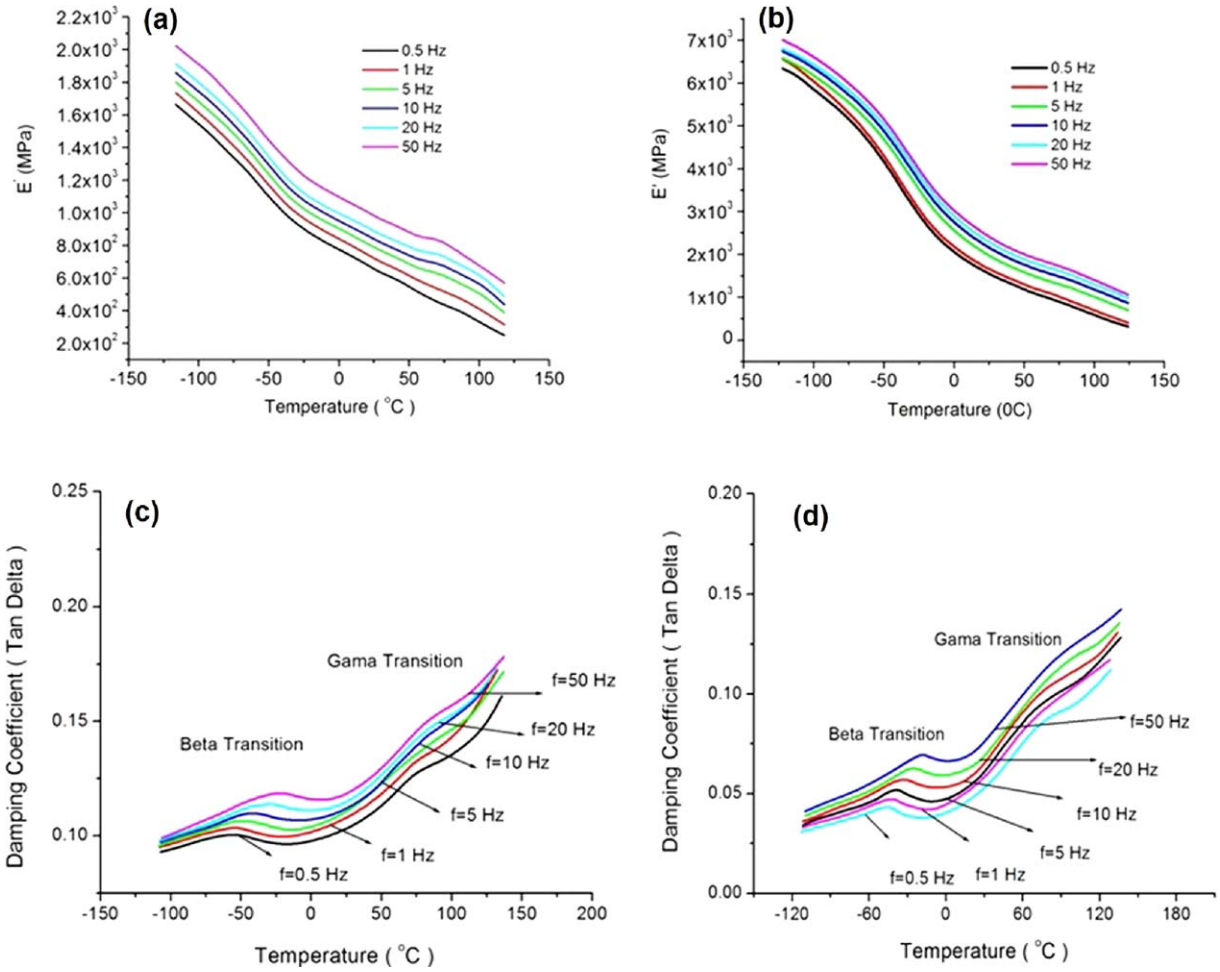

Figure 3. Temperature and frequency dependence of storage modulus, (a) PVDF and (b) nanocomposite and temperature and frequency dependence of tan δ, (c) PVDF and (d) nanocomposite. [Color figure can be viewed in the online issue, which is available at wileyonlinelibrary.com.]

morphology. PVDF powder was gradually added to this solution and the mixing continued for another 12 h under 400 rpm at 25°C until a homogeneous solution was obtained. In this study, 1 wt % of $BaTiO_3$ nanoparticles was added to the matrix. The molding and film fabrication was similar to the aforementioned method.

Characterization

To evaluate the distribution and dispersion of $BaTiO_3$ nanoparticles within PVDF matrix, a Philips CM200 scanning electron microscope and a Philips EM 208S transmission electron microscope were used. The dynamic mechanical analysis (DMA) was performed using a NETZCH-242C instrument in a tension mode on samples at various frequencies in a temperature range of −130°C to +130°C with a heating rate of 5 K/min. The creep recovery cycles were conducted at isotherms between 30 and 110°C at intervals of 20°C. An equilibrium time of 5 min was allowed for each interval before the load was applied. For each isotherm, a constant stress of 0.4 MPa was applied for 30 min, followed by a 30 min recovery period. Frequency sweep tests were conducted at isotherms between 0 and 100°C at intervals of 10°C. An equilibrium time of 5 min was allowed for each interval before commencing the frequency sweep. This test was carried out at six different frequencies of 0.5, 1, 5, 10, 20, and 50 Hz.

RESULTS AND DISCUSSION

Morphology

The dispersion of nanoparticles in the polymeric matrix has a significant effect on the mechanical properties of the resultant nanocomposites. The dispersion of inorganic filler in a polymeric matrix is known to be a difficult process. Figure 2(a,b) presents SEM micrograph of $BaTiO_3$ nanoparticles which are very close to each other. It could be attributed to the high cohesion energy between nanoparticles which can cause the formation of nanoparticle clusters in polymer nanocomposite. TEM micrographs in Figure 2(c,d) also show the dispersion state of $BaTiO_3$ nanoparticles in the nanocomposite. As observed, the quality of mixture is reasonably uniform creating a suitable morphology. This desirable morphology was achieved because of probable compatibility between polymer and nanoparticles.[8,9]

Glass Transition Temperature (T_g) and Frequency Relationship

Figures 3(a,b) depicts the storage modulus (E') of the samples. As can be observed, with an increase in the frequency, the

Table I. Variation of Glass Transition Temperature (T_g) Versus of Frequencies for Studied Samples

Samples	Frequency (Hz)	T_g (°C)
PVDF	0.5	−52.74
	1	−50.62
	5	−46.85
	10	−39.74
	20	−28.32
	50	−22.03
Nanocomposite	0.5	−46.09
	1	−42.65
	5	−39.47
	10	−32.98
	20	−25.58
	50	−19.63

storage modulus increased for all of the samples. It is the desirable outcome, as the relaxation time of the polymer chains stress increased with frequency. The dissipation factor changes in the samples against frequency and temperature are depicted in the same figure. Because of the viscoelastic behavior of polymers, T_g is highly dependent on the frequency. The dissipation factor provided important information about T_g. Due to their viscoelastic nature, T_g of polymers depends on the variations of frequency. The T_g values of samples were estimated from Figure 3(c,d) and presented in Table I. Comparing these dissipation figures of the samples, it is shown that T_g increased with frequency in both samples.

Increase in frequency means a decrease in time resulting in lack of sufficient energy for relaxation time for the polymer chains.[15,16] The relaxation time is viable at higher temperatures, hence, the chains preference to achieve the relaxation time at higher temperatures. A comparison between T_g values at a constant frequency reveals that T_g of nanocomposite is higher than that of neat polymer.[15] The nanoparticles reduced the free volume between the chains by hampering their free movements, therefore, increased their relaxation time at higher temperatures. Moreover, it was observed that the amount of dissipation in nanocomposites decreased in relation to the neat polymer because of the aforementioned reasons.

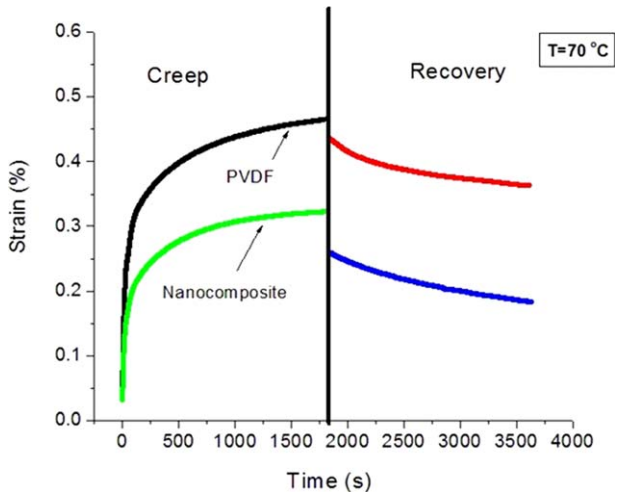

Figure 4. Strain response to creep and recovery cycle at 70°C for PVDF and PVDF/$BaTiO_3$ nanocomposite. [Color figure can be viewed in the online issue, which is available at wileyonlinelibrary.com.]

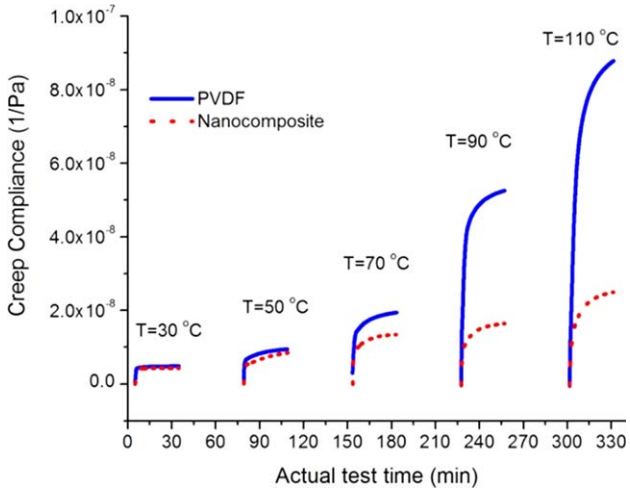

Figure 5. Creep compliance at different temperatures for the PVDF and PVDF/$BaTiO_3$ nanocomposite. [Color figure can be viewed in the online issue, which is available at wileyonlinelibrary.com.]

Creep Test Analysis

The creep and recovery results for the PVDF sample and nanocomposite at 70°C are shown in Figure 4. It is observed that when a constant load was applied to the samples in the creep section, a deformation occurred instantaneously, which was related to the elastic part of the samples. Both samples strained. The strain rate in the nanocomposite sample was lower than that of the neat polymer. It is owing to the less viscous properties of nanocomposite sample. Removing the stress from the samples, it was observed that an abrupt strain was created which was greater for nanocomposite sample. It shows that

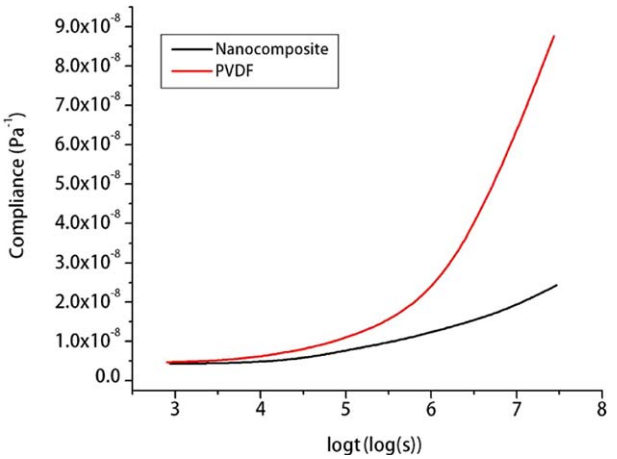

Figure 6. The master curves generated from shifted creep compliances data for PVDF and PVDF/$BaTiO_3$ nanocomposite. [Color figure can be viewed in the online issue, which is available at wileyonlinelibrary.com.]

Table II. Storage and Creep Modulus at Different Temperature and Time

Samples	E' at 20°C (MPa)	E' at 30°C (MPa)	Modulus at 1 year (MPa)	Modulus at 10 years (MPa)
PVDF	682.11	636.34	90.9	40.2
Nanocomposites	1644.24	1469.34	173	161

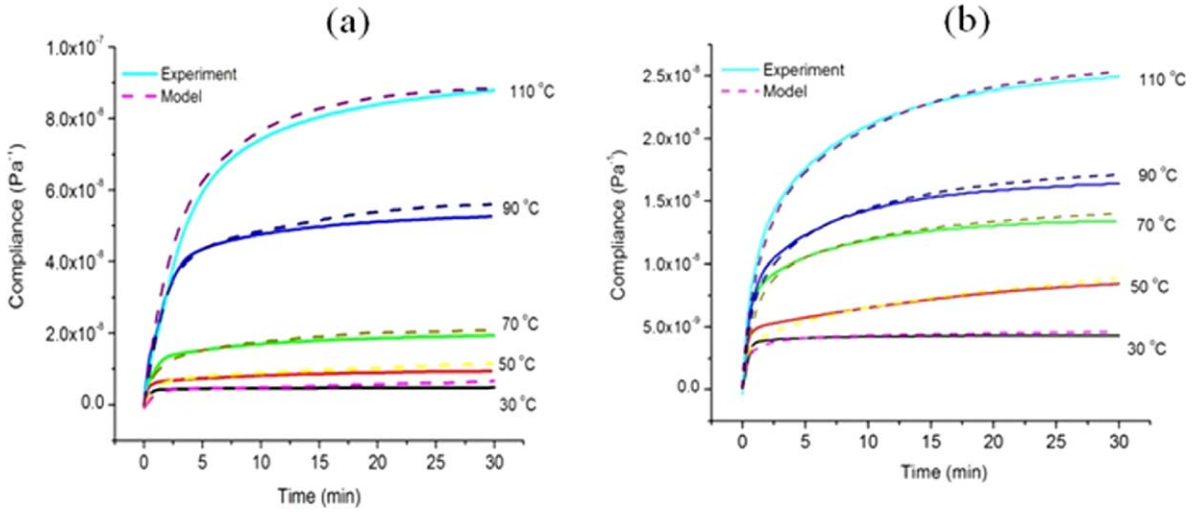

Figure 7. Plots the experimental creep and fitting Burger model (a) PVDF and (b) PVDF/$BaTiO_3$ nanocomposite. [Color figure can be viewed in the online issue, which is available at wileyonlinelibrary.com.]

greater strain was recovered from this sample. By continuing the test, the created strain in the samples was recovered and by the end of the test, the permanent strain that remained in the samples was greater due to the viscous properties of the neat sample.

Temperature change has important effects on the elastic and viscous properties of the material. Figure 5 demonstrates the creep compliance of the studied samples at various times and temperatures.

The cuts in the data in this figure correspond to the recovery and equilibrium times for reaching the isotherm state. Figure 5 also shows that creep compliance of the nanocomposite is smaller in relation to the neat polymer. This phenomenon indicates that nanoparticles reduce the chains movement. Increase in temperature provides the sufficient energy for the chains movements, resulting in more strain. The master curve at the reference temperature of 30°C can be supported by theoretical discussion, TTS, and WLF. Figure 6 shows the reference creep compliance of the studied samples based on logarithmic time (30°C) scale.

Figure 6 illustrates the shifted time in the master creep from eq. (7) using the TTS parameters. Therefore, the creep compliance can be predicted at 30°C for the studied samples. The dotted

Table III. Parameters Obtained from Burger Model

Samples	T (°C)	E_1 (MPa)	E_2 (MPa)	$\eta_1\left(\times 10^{12}\mathrm{Pa\,s}\right)$	τ(s)
PVDF	30	1200	280	1	100
	50	750	150	0.5	120
	70	650	65	0.4	140
	90	420	22	0.24	153
	110	220	14	0.11	165
Nanocomposite	30	1500	310	2.1	50
	50	1100	250	0.42	62
	70	920	110	0.44	75
	90	800	90	0.34	87
	110	620	60	0.21	95

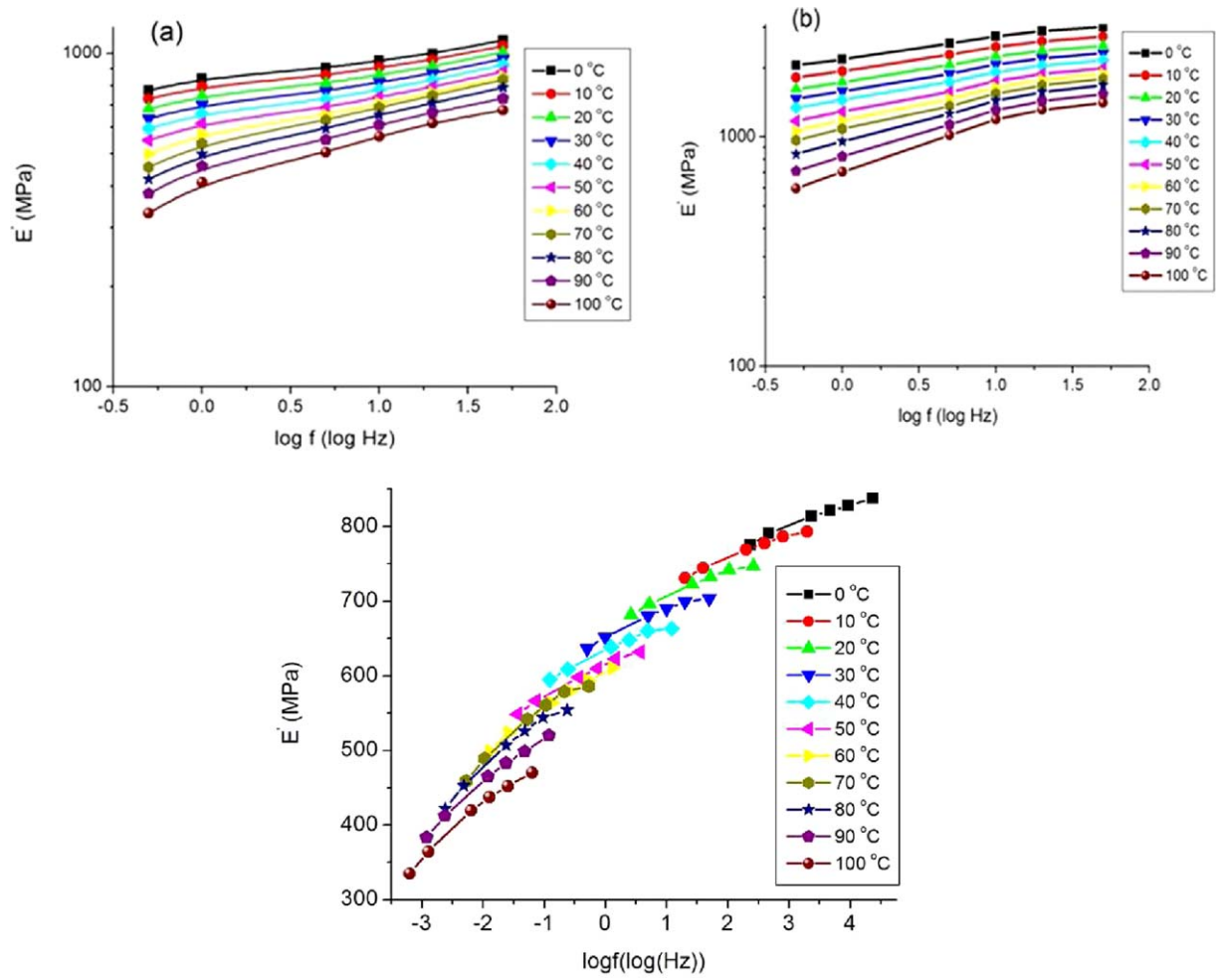

Figure 8. Frequency sweep data versus storage modulus (a) PVDF and (b) PVDF/$BaTiO_3$ nanocomposite, and (c) transferred plot of storage modulus of PVDF at a reference temperature of 30°C. [Color figure can be viewed in the online issue, which is available at wileyonlinelibrary.com.]

lines shown in this figure correspond to 1 and 10 years. Comparing the creep compliance, one can gain a proper understanding of the effect of time on creep compliance of the samples. Thus, it can be deduced that nanocomposite can hold the mechanical properties in a longer time compared to the neat PVDF. The decreased rate of creep compliance with time for the nanocomposite is less than that for the neat PVDF. The values of the storage modulus at different temperatures from DMA and the creep modulus at 1 and 10 years are calculated and presented in Table II.

As previously mentioned in the theoretical background section, we used the Burger's model to obtain the viscoelastic parameters. Fitting the Burger's model to creep data, the elastic and viscous parameters could be obtained at different thermal conditions. Figure 7(a,b) depicts the plots of creep compliances against time at each temperature for experimental data and the Burger's model, simultaneously.

A comparison between the data in this figure reveals that temperature has an important role in creep behavior of the samples. Increase in temperature leads to an increase in creep compliance suggesting an increase in the viscous part and a decrease in the elastic part. On the other hand, the creep compliance behavior of the nanocomposite improved in comparison to the neat sample. It indicates the positive effect of nanoparticles on mechanical properties of the nanocomposite sample, i.e., a decrease in creep compliance. Table III represents a report on the parameters from fitting the Burger's model to experimental data at different thermal conditions.

Generally, increase in temperature reduced the elasticity and increased the retardation time of the modulus in both samples. It indicates that the viscous effects increased with temperature. Furthermore, the comparison between the data on both samples showed that the elastic modulus of the nanocomposite sample increased and the retardation time decreased. It indicated the restrictive effect of the nanoparticles on chains movement.

Sensitivity to applied frequencies is another characteristic of viscoelastic materials which was mentioned in glass transition temperature (T_g) and frequency relationship section. The storage modulus of these materials, which were obtained using the DMTA analysis, is a function of frequency and temperature. Figure 8 presents the change in the PVDF storage modulus at a range of temperatures and frequencies. The nanocomposite manifests the same trend. As observed, increase in temperature and frequency reveals inverse effects on the storage modulus.

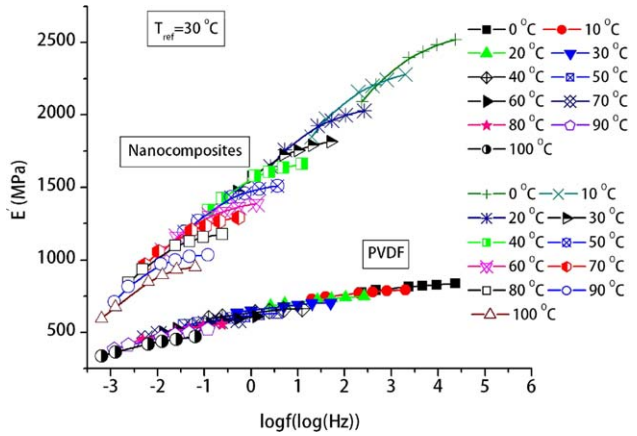

Figure 9. Frequency dependent master curves generated from shifted data for PVDF and PVDF/$BaTiO_3$ nanocomposite. [Color figure can be viewed in the online issue, which is available at wileyonlinelibrary.com.]

Increase in temperature and frequency reduced and increased the storage modulus, respectively. The increase in temperature provides the sufficient energy for chains to overcome the movement barriers and therefore softens the material. On the other hand, increase in the frequency meant a decrease in the relaxation time of the polymer chains hence impeding their movement and increasing the storage modulus. To investigate the behavior of the material at higher frequencies, we could utilize the TTS principle. Figure 8 shows the master curve for PVDF at the reference temperature (30°C), as an example.

Figure 9 shows master curves of storage modulus against frequency generated from manually shifted data at the reference temperature of 30°C for both samples. As observed, increase in frequency resulted in an increase in the storage modulus which was more noticeable for nanocomposite sample, and in a certain frequency, the storage modulus of the nanocomposite was a few times greater than that of the neat polymer sample.

CONCLUSIONS

Comparing the dissipation figures, it can be observed that an increase in the frequency caused an increase in the glass transition temperature. The T_g of the nanocomposite in a fixed frequency was higher than the neat polymer, comparatively. As a result, the amount of the dissipation factor for the nanocomposite was smaller than that of the neat polymer sample. The results of the creep test in different temperatures showed that the nanocomposite sample has a lower strain and creep compliance in comparison with the neat polymer. Comparing the data on both samples, it was observed that the nanocomposite effectively maintains its mechanical properties with the creep compliance rate much less than that of the neat polymer sample, at longer periods. Consequently, nanocomposite showed smaller modulus drop in comparison with the neat sample in periods from 1 to 10 years. Fitting the creep data to the Burger's model, the elastic and viscous parameters of the samples were obtained in different thermal conditions. In general, increase in temperature in both samples reduced the elasticity of the modulus and increased the retardation time. It revealed an increase in the viscous effect in the samples following an increase in the temperature. Furthermore, the investigation of the effect of frequency at different temperatures for the samples showed that the storage modulus is a function of the applied temperature and frequency both, in a manner that an increase in the frequency and temperature will increase and decrease the storage modulus, respectively. To investigate the storage modulus behavior of the samples in much higher and lower frequencies, the TTS equation was used and a master curve was obtained for the storage modulus against the frequency. It was shown that the storage modulus increased with frequency. This effect was more prominent for nanocomposite sample and at a certain frequency, the storage modulus of the nanocomposite was a few order greater than that of the neat polymer.

ACKNOWLEDGMENTS

The authors thank Tarbiat Modares University and the Iranian Nanotechnology Initiative for their support.

REFERENCES

1. Shirinov, A. V.; Schomburg, W. K. *Sens. Actuat. Phys.* **2008**, *142*, 48.
2. Castagnet, S.; Gacougnolle, J. L.;, Dang, P. *Mater. Sci. Eng.* **2000**, *276*, 152.
3. Mano, J. F.; Sencadas, V.; Costa, A. M.; Lanceros-Méndez, S. *Mater. Sci. Eng.* **2004**, *370*, 336.
4. Achaby, M. E.; Arrakhiz. F. Z.; Vaudreuil, S.; Essassi, E. M.; Qaiss, A.; Bousmina, M. *J. Appl. Polym. Sci.* **2013**, *127*, 4697.
5. Zak, A. K.; Gan, W. C.; Abd, W. H.; Darroudi, M.; Velayutham, T. S. *Ceram. Inter.* **2011**, *37*, 1653.
6. Tang, X. G.; Hou, M.; Ge, L.; Zou, J.; Truss, R.; Yang, W.; Yang, M. B.; Zhu, Z. H.; Bao, R. Y. *J. Appl. Polym. Sci.* **2012**, *125*, E592.
7. Rekik, H.; Ghallabi, Z.; Royaud, I.; Arous, M.; Seytre, G.; Boiteux, G.; Kallel, A. *Compos.: Part B. Eng.* **2013**, *45*, 1199.
8. Dang, Z.-M.; Wang, H.-Y.; Zhang, Y.-H.; Qi, J.-Q. *Macromol. Rapid. Commun.* **2005**, *26*, 1185.
9. Mendes, S. F.; Costa, C. M.; Caparros, C.; Sencadas, V.; Lanceros-Méndez, S. *J. Mater. Sci.* **2012**, *47*, 1378.
10. Tang, X. G.; Hou, M.; Zou, J.; Truss, R.; Zhu, Z. *Compos. Sci. Tech.* **2012**, *72*, 1656.
11. Nielsen, L. E.; Landel, R. F. Mechanical Properties of Polymers and Composites, 2nd ed.; Marcel Dekker: New York, **1994**.
12. Genovese, A.; Shanks, R. A. *Macromol. Mater. Eng.* **2007**, *292*, 184.
13. Hiemenz, P. C. Polymer Chemistry: The Basic Concepts; Marcel Dekker: New York, **1984**.
14. Rudin, A. Polymer Science and Engineering, 2nd ed., Academic Press: New York, **1999**.
15. Lim, S. K.; Lim, S. T.; Kim, H. B.; Chin, I.; Choi, H. J. *J. Macromol. Sci. B.* **2003**, *42*, 1197.
16. Sperling, L. H. Introduction to Physical Polymer Science, 4th ed., Wiley: New York, **2006**.